

# Ir(III) Complexes based on Quinoline Carboxamide Ligands for CO<sub>2</sub> Hydrogenation and Formic Acid Dehydrogenation in Water

Soumyadip Patra<sup>a</sup>, Yuichiro Himeda<sup>\*a</sup>

<sup>a</sup> Global Zero Emission Research Center, National Institute of Advanced Industrial Science and Technology Tsukuba West, 16-1 Onogawa, Tsukuba, Ibaraki, 305-8569, Japan

E-mail: himeda.y@aist.go.jp

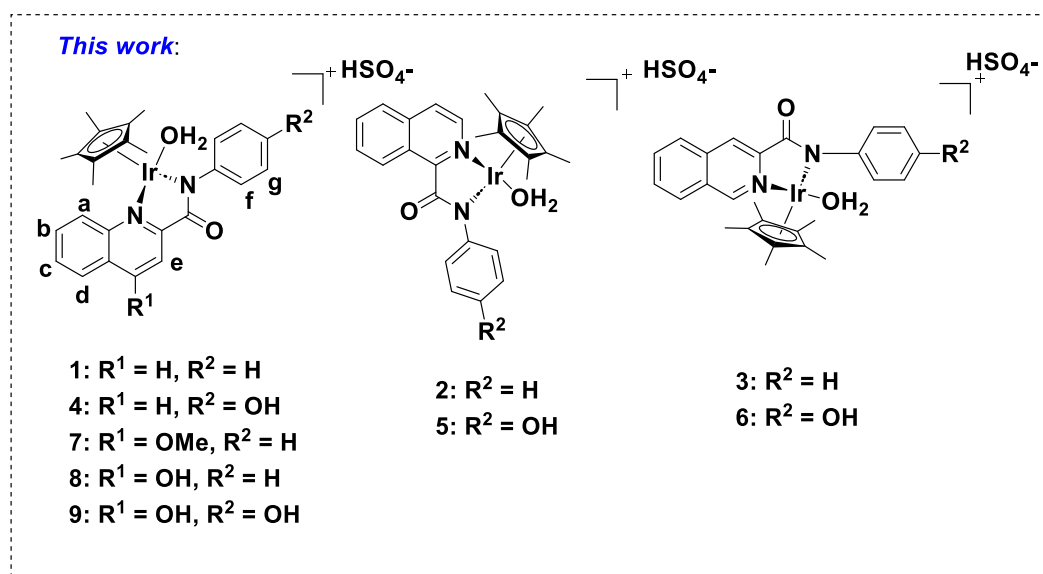
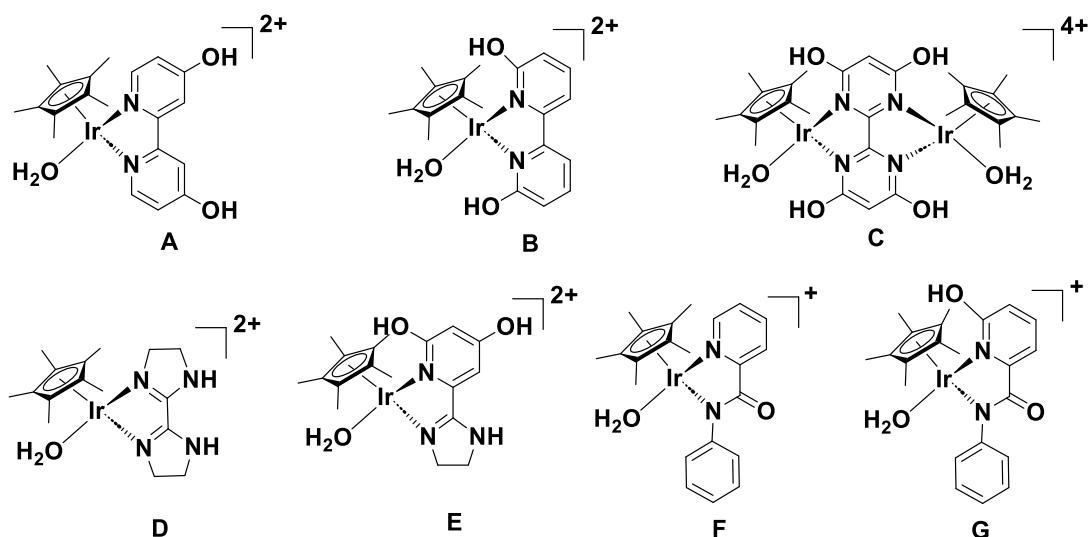
## Abstract

A series of new quinoline and isoquinoline carboxamide based Ir(III) complexes based on the concept of strong electron donating ability of the anionic N-atom have been developed for hydrogenation of CO<sub>2</sub> and dehydrogenation of formic acid (FADH) in water. The effect in catalytic activities with the series of complexes differing in the position of the quinoline ring as well as electron donating methoxy (-OMe) and hydroxy (-OH) functional groups has been investigated in detail. The complex **9** bearing the ligand 4-hydroxy-N-(4-hydroxyphenyl)quinoline-2-carboxamide was found to be the most efficient in CO<sub>2</sub> hydrogenation with a TOF of 2040 h<sup>-1</sup> at 50 °C and 1 MPa H<sub>2</sub>/CO<sub>2</sub> (1:1) pressurized conditions. The active catalyst **9** exhibited an initial TOF of 75 h<sup>-1</sup> for CO<sub>2</sub> hydrogenation even under ambient temperature and pressure in basic aqueous solution. In FADH, the complex **2** bearing the ligand N-phenyl isoquinoline-1-carboxamide had the highest catalytic activity with the initial TOF > 26000 h<sup>-1</sup> for 1 M formic acid (FA) solution (pH 1.7) at 60 °C and achieving initial TOF up to 115000 h<sup>-1</sup> for 8 M FA solution at 80 °C.

## Introduction

The exponential growth in the global population clubbed with modernization and higher standards of living over the last two decades have triggered a tremendous increase in the demand for energy. At present, most of the energy demand is met by the consumption of non-renewable fossil fuel reserves as a result of which a significant amount of CO<sub>2</sub> and other greenhouse gases have been released into the environment. The presence of such gases over an optimal limit in the atmosphere leads to global warming which in turn has multiple adverse climatic effects. Thus, the continuously depleting fossil fuel reserves together with its adverse climatic implications calls for the need of alternate, clean and renewable energy source to fulfil

the demand of a modern and sustainable society.<sup>[1]</sup> Despite CO<sub>2</sub> being a major greenhouse gas, it is also considered as an useful and renewable C1 source which can be utilized for the production of useful and fuel pertinent chemicals such as methanol, formic acid and methane.<sup>[2]</sup> The hydrogenation of CO<sub>2</sub> with hydrogen to produce platform C1 chemicals provide an ideal option to address the problem of rising CO<sub>2</sub> levels in the global atmosphere. Notably, CO<sub>2</sub> hydrogenation to formic acid (FA)/formate has received considerable attention recently owing to the application of CO<sub>2</sub> as an energy vector for H<sub>2</sub> storage.<sup>[2b, 2c, 3]</sup> The importance of FA also arises from the fact that it is considered as one of the prime C1 liquid organic hydrogen carriers (LOHCs) from which hydrogen can be released on demand under mild reaction conditions by employing a suitable catalyst.<sup>[2a, 4]</sup> Hydrogen is considered as a promising carbon free energy carrier for our sustainable future provided that we can overcome the limitations regarding its safe storage and transportation.<sup>[5]</sup> For this purpose, the efforts of the research community is extensively invested in designing active catalysts which can generate hydrogen from liquids such as FA due to convenience in their storage and transportation as compared to gaseous hydrogen.<sup>[4a-d]</sup>



**Scheme 1.** Literature known Cp\*-Ir(III) catalysts for CO<sub>2</sub> hydrogenation and formic acid dehydrogenation in water

The direct hydrogenation of CO<sub>2</sub> to FA in the gas phase,  $\text{CO}_2(\text{g}) + \text{H}_2(\text{g}) \rightleftharpoons \text{HCOOH}(\text{l})$  is thermodynamically not favourable ( $\Delta G^\circ = 32.8 \text{ kJ/mol}$ ). However, the addition of a base or amine in aqueous phase makes the hydrogenation reaction  $\text{CO}_2(\text{aq}) + \text{H}_2(\text{aq}) + \text{NH}_3(\text{aq}) \rightleftharpoons \text{HCOO}^-(\text{aq}) + \text{NH}_4^+(\text{aq})$  energetically favourable ( $\Delta G^\circ = -35.4 \text{ kJ/mol}$ ). Thus, basic reaction conditions are necessary for CO<sub>2</sub> hydrogenation owing to the higher stability of the formate salt than that of FA.<sup>[6]</sup> Although some very efficient catalysts have been developed for CO<sub>2</sub> hydrogenation<sup>[7]</sup> and FADH reactions<sup>[8]</sup> separately over the last decade, efficient catalytic systems which can selectively hydrogenate CO<sub>2</sub> to FA/formate and subsequently catalyze the FADH reaction in aqueous medium are of great value in view of a reversible hydrogen storage

and release system with CO<sub>2</sub>.<sup>[9]</sup> In this regard, we had previously investigated the Cp\*Ir catalysts **A** and **B** (Scheme 1) for efficient CO<sub>2</sub> hydrogenation as well as FADH reactions in water.<sup>[8c, 10]</sup> The catalyst design concept was based on the fact that introduction of anionic ligand generated by the deprotonation of a hydroxyl group behave as a proton responsive moiety and improve the catalytic activity via strong electron donation to the metal. Complex **A** catalyzed CO<sub>2</sub> hydrogenation to formate with an initial TOF of 650 h<sup>-1</sup> under P<sub>H<sub>2</sub>/CO<sub>2</sub></sub> (1 MPa) at 50 °C,<sup>[10a]</sup> and FADH with initial TOF: 2400 h<sup>-1</sup> (pH 1.7) at 60 °C.<sup>[8c]</sup> The catalytic activity of complex **B** in CO<sub>2</sub> hydrogenation was found to be much higher than **A**, producing an initial TOF of 1650 h<sup>-1</sup> under analogous reaction conditions as **A**.<sup>[10a]</sup> This enhancement in the catalytic activity was supposed to be due to the exploitation of secondary coordination sphere effect in the catalyst design where the ortho-positioned hydroxyl group accelerates H<sub>2</sub> heterolysis through proton relay with the assistance of a water molecule (pendant base effect). **B** was reported as the first molecular catalyst to catalyze the CO<sub>2</sub> hydrogenation to formate under ambient reaction conditions (25 °C, atmospheric pressure) with a TOF of 27 h<sup>-1</sup>.<sup>[11]</sup> Complex **B** catalyzed FADH with an initial TOF: 5440 h<sup>-1</sup> (pH 3.5) at 60 °C.<sup>[10b]</sup> Subsequently, we reported the tetrahydroxy bipyrimidine Cp\*Ir complex **C** (Scheme 1) in 2012 which displayed much higher activity as compared to its dihydroxy analogues due to a combination of electron rich oxyanion group and pendant base effects. Catalyst **C** displayed a TOF of 4200 h<sup>-1</sup> and 70 h<sup>-1</sup> for CO<sub>2</sub> hydrogenation to formate under P<sub>H<sub>2</sub>/CO<sub>2</sub></sub> (1 MPa) at 50 °C and P<sub>H<sub>2</sub>/CO<sub>2</sub></sub> (0.1 MPa) at 25 °C respectively. A TOF of 31600 h<sup>-1</sup> for FADH (pH 3.5) at 60 °C was achieved with **C**.<sup>[12]</sup> In 2015, we explored the Cp\*Ir complex **D** (Scheme 1) bearing a non aromatic bisimidazoline ligand and achieved a TOF of 1290 h<sup>-1</sup> for CO<sub>2</sub> hydrogenation under P<sub>H<sub>2</sub>/CO<sub>2</sub></sub> (1 MPa) at 50 °C.<sup>[13]</sup> Moreover, **D** was found to exhibit very high activity towards FADH and a TOF: 54700 h<sup>-1</sup> was achieved at pH 1.7.<sup>[14]</sup> Catalyst **D** was designed based on the concept that nonaromatic imidazoline moiety could enhance electron density on the N atom by localization. Subsequently, we reported the complex **E** (Scheme 1) based on pyridyl imidazoline moiety and achieved an initial TOF of 2600 h<sup>-1</sup> for CO<sub>2</sub> hydrogenation to formate under P<sub>H<sub>2</sub>/CO<sub>2</sub></sub> (1 MPa) at 50 °C. Complex **E** could also catalyze the CO<sub>2</sub> hydrogenation reaction at room temperature under atmospheric pressure with an initial TOF of 106 h<sup>-1</sup>. In FADH, a high activity of 56900 h<sup>-1</sup> (pH 3.0) could be achieved with **E**. The high activity of catalyst **E** was attributed to a combination of proton responsive oxyanion groups and the presence of nonaromatic imidazoline moiety.<sup>[15]</sup>

Based on previous reports with complexes bearing amide ligands,<sup>[16]</sup> we explored some Cp\*Ir complexes based on amidate moiety for CO<sub>2</sub> hydrogenation and FADH reactions in

water (**F** and **G** in Scheme 1) and achieved high catalytic activities. Among several structurally similar catalysts explored, complex **G** outperformed others in CO<sub>2</sub> hydrogenation to achieve a record TOF of 198 h<sup>-1</sup> under ambient reaction conditions, due to strong electron donation by the amidate moiety in addition to the oxyanion effect. The same catalyst exhibited a TOF of 3140 h<sup>-1</sup> in CO<sub>2</sub> hydrogenation under pressurized reaction conditions of 1 MPa P<sub>H<sub>2</sub>/CO<sub>2</sub></sub> at 50 °C. In FADH, complex **F** bearing a N-phenyl picolinamidate ligand displayed a TOF of 20800 h<sup>-1</sup> for 1 M FA solution at 60 °C.<sup>[17]</sup> Encouraged by the high catalytic activities achieved with the picolinamidate Cp\*Ir(III) complexes, herein, we report a series of quinoline and isoquinoline carboxamide based Cp\*Ir complexes (**1**–**9**) based on the concept that pK<sub>a</sub> (isoquinoline; 5.46) > pK<sub>a</sub> (pyridine; 5.17) > pK<sub>a</sub> (quinoline; 4.85). The design concept based on the difference in basicity of the ligands bound to the Cp\*Ir led to distinct catalytic activities both in case of CO<sub>2</sub> hydrogenation and FADH reactions. In addition, the effect of electron donating methoxy (-OMe) and hydroxy (-OH) functional groups in the quinoline ring and the N<sub>phenyl</sub> group at the amide-N have also been investigated in detail. The structure-activity relationship could be elucidated by extensive pH and kinetic isotope effect (KIE) studies with selected catalysts.

## Results and Discussion

### Synthesis and Characterization of the Ligands and Complexes

**Table 1.** Chemical shift comparison of specified protons in the  $^1\text{H}$  NMR spectra of complex **9** in (i)  $\text{D}_2\text{O}$  and (ii)  $\text{NaOD}/\text{D}_2\text{O}$ .

Proton	$^1\text{H}$ NMR in $\text{D}_2\text{O}$ $\delta$ (ppm)	$^1\text{H}$ NMR in $\text{NaOD}/\text{D}_2\text{O}$ $\delta$ (ppm)
<b>e</b>	7.39	6.85
<b>g</b>	6.92	6.53
<b>c</b>	8.04	7.73
<b>b</b>	7.77	7.46

The ligands and complexes were synthesized by following the procedure described in the Supporting Information. The newly synthesized  $\text{Cp}^*\text{Ir}$  complexes were characterized by  $^1\text{H}$ ,  $^{13}\text{C}$  NMR and mass spectrometry. The  $^1\text{H}$  NMR spectra of complex **9** in  $\text{D}_2\text{O}$  and  $\text{NaOD}/\text{D}_2\text{O}$  was recorded at room temperature. It was observed that the proton **e** located adjacent to the carbon atom with the  $-\text{OH}$  group displayed the most significant upfield shift in the NMR spectra recorded in  $\text{NaOD}/\text{D}_2\text{O}$ . It appeared as a singlet at  $\delta = 6.85$  ppm in  $\text{NaOD}/\text{D}_2\text{O}$  as compared to  $\delta = 7.39$  ppm in  $\text{D}_2\text{O}$  (Scheme 1, Table 1 and Figures S1 and S2). Additionally, the protons **g** adjacent to the  $-\text{OH}$  group in the  $\text{N}$ phenyl ring also showed considerable upfield shift (**d**;  $\delta = 6.53$  ppm) in  $\text{NaOD}/\text{D}_2\text{O}$  as compared to the spectra in  $\text{D}_2\text{O}$  (**d**;  $\delta = 6.92$  ppm). The protons **c** and **b** also appeared upfield in  $\text{NaOD}/\text{D}_2\text{O}$  as compared to their respective chemical shifts in the NMR spectra recorded in  $\text{D}_2\text{O}$  (Scheme 1 and Table 1). This suggest the formation of electron rich oxyanionic ligand ( $-\text{O}^-$ ) under basic conditions as indicated in our previous reports.<sup>[10a]</sup>

## CO<sub>2</sub> Hydrogenation

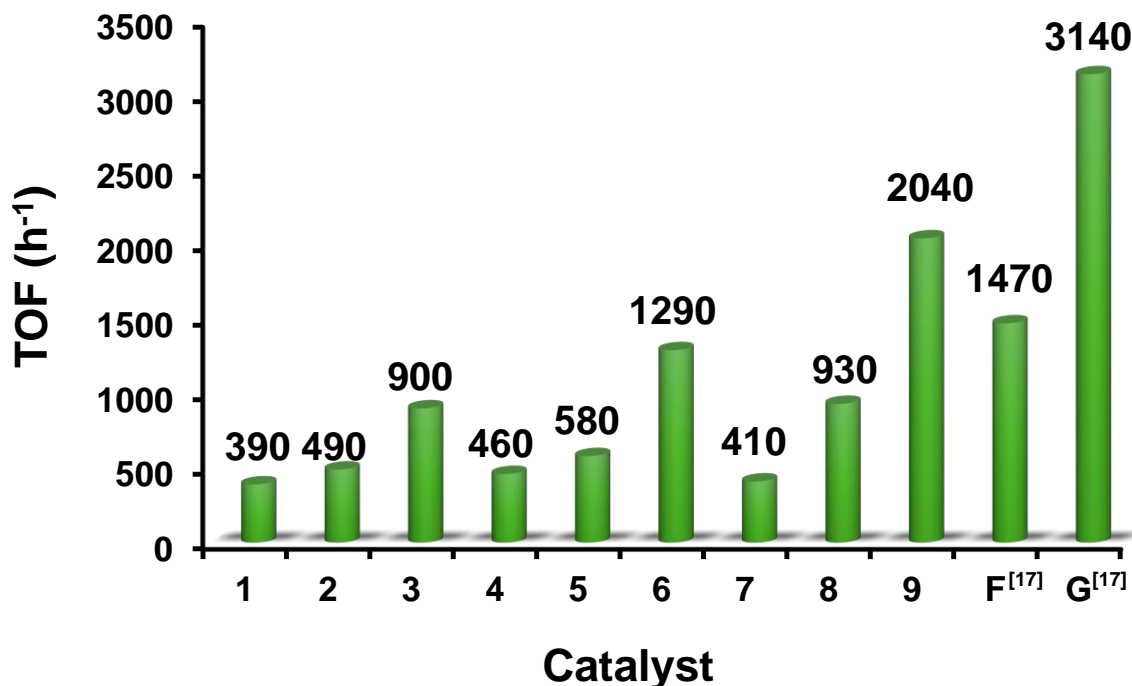


**Figure 1.** Comparative catalytic activity of the complexes **1** – **9**, **F**<sup>[17]</sup> and **G**<sup>[17]</sup> in CO<sub>2</sub> hydrogenation. Reaction Conditions: 1 M NaHCO<sub>3</sub> solution (10 mL) with catalyst (0.2 μmol), P(H<sub>2</sub>/CO<sub>2</sub>) = 1.0 MPa (1/1), reaction time = 1 h, T = 50 °C.

The catalytic activity of the synthesized complexes (**1** – **9**) in CO<sub>2</sub> hydrogenation was systematically investigated to gain insights into the structural and functional group effects of the quinoline carboxamide type ligands (Figure 1). At an outset, **1** with *N*-phenylquinoline-2-carboxamide ligand was examined for CO<sub>2</sub> hydrogenation under pressurized reaction conditions (1.0 MPa H<sub>2</sub>/CO<sub>2</sub> (1/1)), 50 °C, 1 M NaHCO<sub>3</sub>. **1** exhibited a TOF of 390 h<sup>-1</sup> under these reaction conditions. Next, we tested **2** with *N*-phenylisoquinoline-1-carboxamide under analogous reaction conditions and achieved a TOF of 490 h<sup>-1</sup> which shows the incremental effect in the catalytic activity with the more basic isoquinoline type structure as compared to quinoline. Interestingly, the complex **3** with *N*-phenylisoquinoline-3-carboxamide ligand displayed a TOF of 900 h<sup>-1</sup> for CO<sub>2</sub> hydrogenation which was much higher as compared to **1** and **2** under analogous reaction conditions (Figure 1). Subsequently, the effect of hydroxy (-OH) group in the para position of the phenyl group on the amide-N was investigated in detail. **4** with *N*-(4-hydroxyphenyl)quinoline-2-carboxamide exhibited a TOF of 460 h<sup>-1</sup> which was slightly higher as compared to **1**. Similarly, **5** and **6** displayed TOFs of 580 h<sup>-1</sup> and 1290 h<sup>-1</sup>

respectively in CO<sub>2</sub> hydrogenation under analogous reaction conditions which shows the positive effect in catalytic activity exerted by the OH group in the para position of the phenyl group on the amide-N. Next, the effect of the introduction of electron donating methoxy -OMe and OH group on the quinoline ring was investigated. The complex **7** with 5-methoxy-*N*-phenylquinoline-2-carboxamide ligand displayed a TOF of 410 h<sup>-1</sup> under pressurized reaction conditions which shows that the introduction of a methoxy group at the para position of the quinoline ring did not have a significant effect on the catalytic activity. In contrast, the introduction of a OH group at the same position in **8**, afforded a catalytic activity more than two-fold higher as compared to **1** where a TOF of 930 h<sup>-1</sup> was achieved under analogous reaction conditions. This result is in accordance with our previous reports where the introduction of OH groups have proved to be extremely beneficial in achieving high catalytic activity for CO<sub>2</sub> hydrogenation to formate.<sup>[10a, 17]</sup> Next, to understand the effect of OH groups at the para position of both the quinoline ring and the phenyl group on the amide-N, we designed **9** with a 4-hydroxy-*N*-(4-hydroxyphenyl) quinoline-2-carboxamide ligand which exhibited a high TOF of 2040 h<sup>-1</sup> for CO<sub>2</sub> hydrogenation under 1 MPa H<sub>2</sub>/CO<sub>2</sub> (1/1) pressurized conditions at 50 °C (Figure 1). Subsequently, the CO<sub>2</sub> hydrogenation activity of **9** was studied under ambient reaction conditions (0.1 MPa H<sub>2</sub>/CO<sub>2</sub> (1/1)), 25 °C, 1 M NaHCO<sub>3</sub> where an initial TOF of 75 h<sup>-1</sup> was achieved with **9** (Figure S3). The time dependent CO<sub>2</sub> hydrogenation with **9** under ambient reaction conditions revealed that the formate concentration was enhanced with increasing reaction time (Figure S3).



## Formic Acid Dehydrogenation

Entry	Catalyst	FA <sup>[b]</sup>		FA/SF (9/1) <sup>[c]</sup>		FA/SF (1/1) <sup>[d]</sup>	
		Conv. (%) <sup>[e]</sup>	TOF (h <sup>-1</sup> ) <sup>[f]</sup>	Conv. (%) <sup>[e]</sup>	TOF (h <sup>-1</sup> ) <sup>[f]</sup>	Conv. (%) <sup>[e]</sup>	TOF (h <sup>-1</sup> ) <sup>[f]</sup>
1	<b>1</b>	99	9360	88	18960	20	5180
2	<b>2</b>	99	26120	90	16010	30	4670
3	<b>3</b>	99	13800	90	31530	49	14530
4	<b>4</b>	99	18480	63	21430	10	4670
5	<b>5</b>	99	19950	90	38190	45	7390
6	<b>6</b>	99	13550	90	42130	42	19710
7	<b>7</b>	99	11820	61	13055	21	7880
8	<b>8</b>	99	8132	85	5900	20	3600
9	<b>9</b>	99	10602	90	31990	50	16990

[a] Reaction Conditions: Catalyst loading (1  $\mu\text{mol}$ ), T = 60 °C. [b] In a 1 M FA solution (pH 1.7, 10 mL). [c] In a 1 M FA/SF (9/1) solution (pH 2.8, 10 mL). [d] In a 1 M FA/SF (1/1) solution (pH 3.75, 10 mL). [e] determined by HPLC. [f] TOF was calculated from average rate after initial 5 min. All numbers are average of two runs.

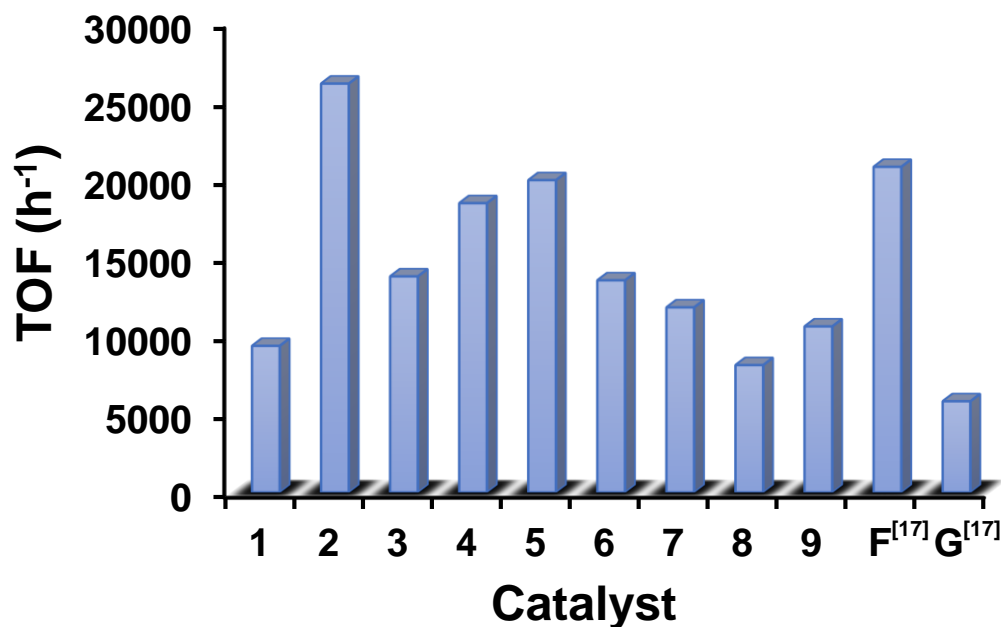


**Figure 2.** Comparative catalytic activity of the complexes **1 – 9**, **F**<sup>[17]</sup> and **G**<sup>[17]</sup> in formic acid dehydrogenation. Reaction conditions: 1 M FA solution (pH 1.7, 10 mL), catalyst (1  $\mu\text{mol}$ ), T = 60 °C, initial TOFs (5 min) .

The results of FADH with **1** – **9** at three different pH conditions: pH 1.7 (1 M FA), pH 2.8 (FA/SF (9/1)) and pH 3.75 (FA/SF (1/1)) are summarized in Table 2. An initial TOF of 9360 h<sup>-1</sup> was achieved with **1** which increased to 18960 h<sup>-1</sup> when a (FA/SF (9/1)); pH 2.8) solution was used. The TOF drastically decreased to 5180 h<sup>-1</sup> with **1** for the (FA/SF (1/1); pH 3.75) solution where very less conversion of formic acid was observed under this reaction condition (entry 1). Next, **2** exhibited almost 3-fold higher catalytic activity for 1 M FADH (pH 1.7) as compared to **1**. A high TOF of 26120 h<sup>-1</sup> in FADH was achieved with **2** at 60 °C which puts it among the highly active molecular catalysts reported for FADH (Figure 2). Notably, only the Cp\*Ir catalysts reported by Li *et al.* are reported to exhibit a higher catalytic activity than **2** under analogous reaction conditions.<sup>[8h, 8l]</sup> The GC analysis of the released gas mixture revealed an equimolar ratio of H<sub>2</sub>:CO<sub>2</sub> with no CO contamination (detection limit: 10 ppm) (Figure S4). Interestingly, the TOF of **2** decreased to 16010 h<sup>-1</sup> with (FA/SF (9/1); pH 2.8) solution and further deteriorated to 4670 h<sup>-1</sup> with (FA/SF (1/1); pH 3.75) solution (entry 2). The structural analogue **3** displayed a TOF of 13800 h<sup>-1</sup> for FADH at pH 1.7 but was greatly influenced by slight increase in the pH, where, a TOF of 31530 h<sup>-1</sup> was achieved with (FA/SF (9/1); pH 2.8) solution. At pH 3.75, **3** exhibited a TOF of 14530 h<sup>-1</sup> and much higher conversion of formic acid was found as compared to **1** and **2** under this reaction condition (entry 3). Thus, a systematic study of **1**, **2** and **3** in FADH at different pH revealed a distinct structure activity behaviour of the quinoline/isoquinoline carboxamide coordinated Cp\*Ir complexes. Moreover, it is worthy to note that the catalytic activity of the complexes **1**, **2** and **F**<sup>[17]</sup> in FADH follow the order **1** < **F** < **2** which is in accordance with the pKa trend (isoquinoline) > (pyridine) > (quinoline) with the Nphenyl moiety remaining same for all the cases. Subsequently, to check the effect of an electron donating OH group in the para position of the N-phenyl ring, we investigated the complexes **4**, **5** and **6** for FADH. **4** displayed a TOF of 18480 h<sup>-1</sup> at pH 1.7 which was 2-fold higher as compared to **1** under analogous reaction conditions. The TOF with **4** increased slightly to 21430 h<sup>-1</sup> at pH 2.8 and deteriorated to 4670 h<sup>-1</sup> at pH 3.75 following the same trend as **1** (entry 4). **5** did not exhibit an incremental catalytic activity as compared to **2** at pH 1.7 but displayed a much higher TOF of 38190 h<sup>-1</sup> at pH 2.8 (entry 5). **6** exhibited a TOF of 13550 h<sup>-1</sup> at pH 1.7 and a slight increase in pH to 2.8 influenced its catalytic activity significantly, where, a TOF of 42130 h<sup>-1</sup> was achieved (entry 6). This trend was similar to that observed in case of **3** but a even higher TOF could be achieved with **6** at pH 2.8. A TOF of 19710 h<sup>-1</sup> was observed with **6** even at higher pH with 1 M (FA/SF (1/1)) solution. Subsequently, we checked the effect of the introduction of electron donating -OMe and -OH groups at the

para position of the quinoline ring. **7** exhibited a TOF of 11820 h<sup>-1</sup> with 1 M FA solution (pH 1.7) which was slightly higher as compared to **1**. The catalytic activity of **7** was not significantly influenced by increasing the pH of the reaction solution to 2.8 (entry 7). Introduction of a OH group in the quinoline ring **8**, did not have a positive effect in the catalytic activity for FADH (entry 8). **9** with OH groups both at the para position of the quinoline ring and the phenyl group on amide-N displayed a TOF of 31990 h<sup>-1</sup> with 1 M (FA/SF (9/1); pH 2.8) solution and 16990 h<sup>-1</sup> with 1 M (FA/SF (1/1); pH 3.75) solution, where, almost full conversion of formic acid was achieved under these reaction conditions (entry 9).

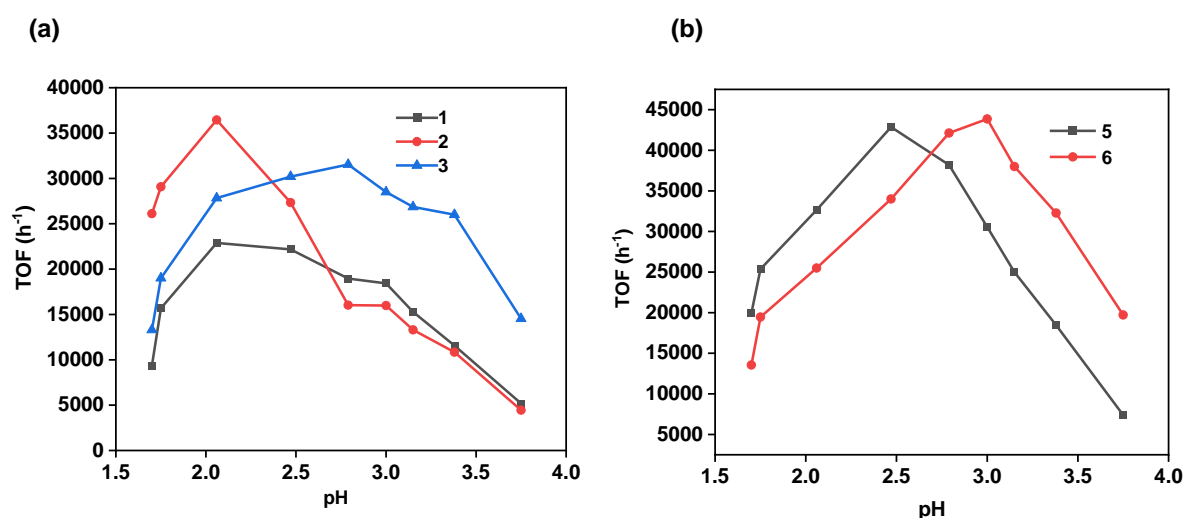


**Figure 3.** Effect of pH on dehydrogenation of FA at 60 °C using (a) **1** (0.1 mM, black square), **2** (0.1 mM, red circle) and **3** (0.1 mM, blue triangle), (b) **5** (0.1 mM, black square) and **6** (0.1 mM, red circle). The pH of the solutions were varied by using solutions of different FA/SF ratios. All reaction volumes were 10 mL. TOFs were calculated from average rates after the initial 5 min.

Subsequently, we examined the detailed pH-dependence of the catalytic activities of **1**, **2** and **3** (Figure 3a and Table S2). From figure 3a, it is evident that **1** and **2** exhibited maximum TOF of 22890 h<sup>-1</sup> and 36450 h<sup>-1</sup> respectively at pH 2.0 where as for **3**, the maximum TOF value of 31536 h<sup>-1</sup> was observed at pH 2.8. The catalytic activity of **2** was very sensitive to changes in pH as the TOF declined sharply with a small increase in pH from 2.0 to 2.8. The TOFs achieved with **3** above pH 2.5 were much higher as compared to **1** and **2**. We also investigated the pH-dependence of the active catalysts **5** and **6** (Figure 3b). **5** exhibited a maximum TOF of 42870 h<sup>-1</sup> at pH 2.5 where as in the case of **6**, the maximum TOF of 43855 h<sup>-1</sup> was observed at a shifted pH of 3.0. The temperature dependent catalytic activity of the most active catalyst **2**

(1 M FA; pH 1.7) was studied in the range of 50 °C to 65 °C (Figure S5a). From the temperature dependent TOFs, it is evident that the catalytic activity of **2** was enhanced with the increase in temperature and an activation energy of 65.9 kJ/mol was calculated from the Arrhenius plot (Figure S5b). Subsequently, we studied the effect of FA concentration on the catalytic activity of **2** (Figure S6 and Table S3). The catalytic activity was enhanced with the increase in FA concentration from 1 M to 6 M and a high TOF of 49446 h<sup>-1</sup> was achieved with 6 M FA solution at 60 °C. Complete conversion of FA was observed with solutions up to 4 M, while for 6 M FA solution, 91 % conversion was observed with **2**. **2** exhibited a high initial TOF of 114457 h<sup>-1</sup> for 8 M FADH at 80 °C without any additive, but only 65 % conversion of FA was found under this reaction condition. A TON of 100000 could be achieved with **2** (1 μmol) in the dehydrogenation of FA (2M, 50 mL) at 60 °C (Figure S7)

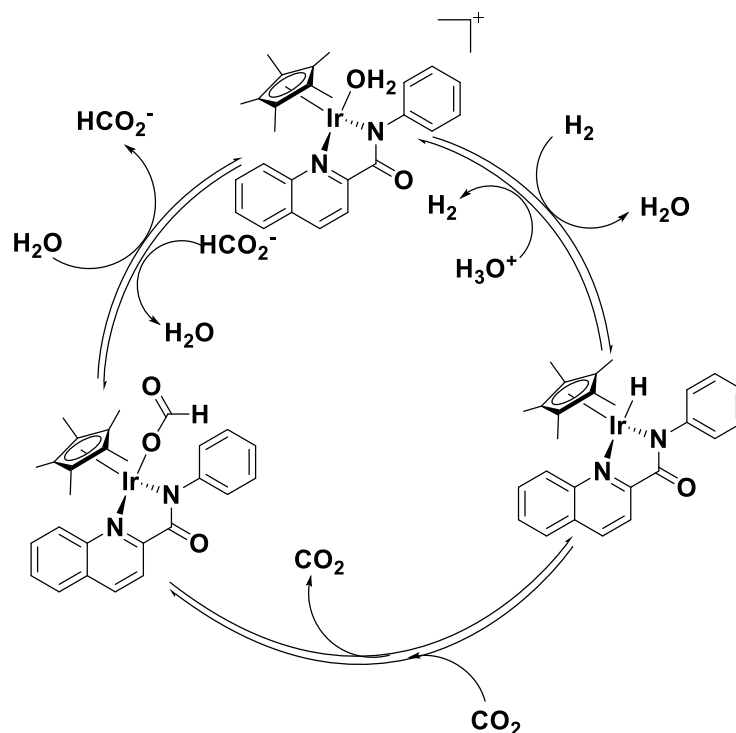
**Table 3.** Experimental Deuterium Kinetic Isotope Effects (KIEs) for FADH by catalysts **1**, **2** and **3**<sup>[a]</sup>

Substrate/Solvent	<b>1</b>		<b>2</b>		<b>3</b>	
	TOF/h <sup>-1</sup>	KIE	TOF/h <sup>-1</sup>	KIE	TOF/h <sup>-1</sup>	KIE
HCOOH/H <sub>2</sub> O <sup>[b]</sup>	8620		23036		12193	
HCOOH/D <sub>2</sub> O <sup>[c]</sup>	4310	2	10223	2.25	7018	1.74
DCOOD/H <sub>2</sub> O <sup>[d]</sup>	5050	1.71	9482	2.43	3693	3.30
DCOOD/D <sub>2</sub> O <sup>[e]</sup>	2950	2.92	3942	5.84	2094	5.82

[a] Reaction Conditions: Catalyst (1 μmol), temperature (60 °C), initial TOFs (10 min)  
 [b] 1 M HCOOH/H<sub>2</sub>O (10 mL), [c] 1 M HCOOH/D<sub>2</sub>O (10 mL), [d] 1 M DCOOD/H<sub>2</sub>O (10 mL), [e] 1 M DCOOD/D<sub>2</sub>O (10 mL).

The KIE studies conducted with the catalysts **1**, **2** and **3** revealed a very interesting trend for the structure activity relationship among them (Table 3). For **1**, HCOOH in D<sub>2</sub>O was found to be more influential than DCOOD in H<sub>2</sub>O indicating that the proton assisted hydrogen release might be the rate determining step (RDS) in the catalytic cycle of FADH. Interestingly, for **2** and **3**, DCOOD in H<sub>2</sub>O was found to be more influential than HCOOH in D<sub>2</sub>O indicating that the decarboxylation step might be the RDS in the catalytic cycle. For **1** and **2**, the difference in KIE values of HCOOH in D<sub>2</sub>O and DCOOD in H<sub>2</sub>O were close which explains the similar behaviour of their pH-dependent catalytic activities while in the case of **3**, the KIE value of DCOOD in H<sub>2</sub>O was significantly higher than HCOOH in D<sub>2</sub>O explaining the higher catalytic activities displayed by **3** at a slightly higher pH as compared to **1** and **2**. Based on our findings, the plausible reaction pathway for dehydrogenation of FA over the studied catalytic system

may involve the following sequential steps: (a) Ir-formato species is formed by replacement of H<sub>2</sub>O with formate in the solution, (b) decarboxylation of the Ir-formato intermediate results in the generation of Ir-H species, and (c) finally, hydrogen is released from the Ir-H to regenerate the original Ir-aqua complex. For CO<sub>2</sub> hydrogenation, (a) Ir-H species is generated in H<sub>2</sub> atmosphere, (b) insertion of CO<sub>2</sub> into the Ir-H leads to the formation of Ir-formato species and (c) finally the formate is released into the solution to regenerate the Ir-aqua complex and complete the catalytic cycle (Scheme 2).



**Scheme 2.** A plausible reaction mechanism for CO<sub>2</sub> hydrogenation (outside circle) and FADH reactions (inside circle) with representative complex **1**.

## Conclusions

In summary, a series of quinoline/isoquinoline carboxamidate based Cp\*Ir complexes were synthesized and explored for CO<sub>2</sub> hydrogenation as well as FADH reactions in water. The effect of structure of the quinoline/isoquinoline ring as well as electron donating methoxy and hydroxy functional groups on the catalytic activities in CO<sub>2</sub> hydrogenation and FADH was extensively investigated by performing the reactions at different pH and KIE experiments. The catalyst **9** was the most efficient in CO<sub>2</sub> hydrogenation and displayed a TOF of 2040 h<sup>-1</sup> and 75 h<sup>-1</sup> for CO<sub>2</sub> hydrogenation to formate under P<sub>H<sub>2</sub>/CO<sub>2</sub></sub> (1 MPa) at 50 °C and P<sub>H<sub>2</sub>/CO<sub>2</sub></sub> (0.1 MPa) at 25 °C respectively. The formation of the oxyanion ligand (O<sup>-</sup>) under basic reaction conditions

was attributed to the high catalytic activity of **9**. In FADH, complex **2** was found to display the highest catalytic activity of 26120 h<sup>-1</sup> for 1 M FA solution (pH 1.7) at 60 °C. The observed catalytic activities among Cp\*Ir complexes **1**, **2** and **F** in FADH is found to be in accordance with the pKa values of quinoline, pyridine and isoquinoline structures. The isoquinoline structure with higher pKa value as compared to quinoline was more beneficial for FADH most likely due to higher electron donation to the Ir center. Moreover, the presence of an electron donating OH group in the para position of the *N*-phenyl ring (**4**, **5** and **6**) had significant influence on the catalytic activities for FADH at different pH values. KIE studies indicated that the proton assisted hydrogen release step is the RDS in FADH with **1**, while the decarboxylation step could be the RDS with **3**. We hope that our present findings related to the structure activity relationship of Cp\*Ir amidate complexes in CO<sub>2</sub> hydrogenation and FADH reactions will pave the way for the development of more active and robust molecular catalysts for reversible hydrogen storage/release application in the near future.

## Acknowledgements

## References

- [1] M. S. Dresselhaus, I. L. Thomas, *Nature* **2001**, *414*, 332-337.
- [2] a) M. Grasmann, G. Laurency, *Energy Environ. Sci.* **2012**, *5*, 8171-8181; b) J. Klankermayer, S. Wesselbaum, K. Beydoun, W. Leitner, *Angew. Chem Int. Ed.* **2016**, *55*, 7296-7343; c) W.-H. Wang, Y. Himeda, J. T. Muckerman, G. F. Manbeck, E. Fujita, *Chem. Rev.* **2015**, *115*, 12936-12973; d) S. Kar, J. Kothandaraman, A. Goepfert, G. K. S. Prakash, *Journal of Co2 Utilization* **2018**, *23*, 212-218; e) S. Zhang, Q. Fan, R. Xia, T. J. Meyer, *Acc. Chem. Res.* **2020**, *53*, 255-264; f) S. Kar, A. Goepfert, G. K. S. Prakash, *Acc. Chem. Res.* **2019**, *52*, 2892-2903; g) A. Kumar, P. Daw, D. Milstein, *Chem. Rev.* **2022**, *122*, 385-441.
- [3] K. Sordakis, C. Tang, L. K. Vogt, H. Junge, P. J. Dyson, M. Beller, G. Laurency, *Chem. Rev.* **2018**, *118*, 372-433.
- [4] a) D. Mellmann, P. Sponholz, H. Junge, M. Beller, *Chem. Soc. Rev.* **2016**, *45*, 3954-3988; b) J. Eppinger, K.-W. Huang, *ACS Energy Lett.* **2017**, *2*, 188-195; c) C. Guan, Y. Pan, T. Zhang, M. J. Ajitha, K.-W. Huang, *Chem. - Asian J.* **2020**, *15*, 937-946; d) N. Onishi, R. Kanega, H. Kawanami, Y. Himeda, *Molecules* **2022**, *27*; e) M. X. Liu, Y. K. Xu, Y. Meng, L. J. Wang, H. Wang, Y. C. Huang, N. Onishi, L. Wang, Z. J. Fan, Y. Himeda, *Adv. Energy Mater.* **2022**, *12*.
- [5] a) J. A. Turner, *Science* **2004**, *305*, 972-974; b) G. M. Whitesides, G. W. Crabtree, *Science* **2007**, *315*, 796-798; c) P. Moriarty, D. Honnery, *Int. J. Hydrogen Energy* **2009**, *34*, 31-39; d) N. S. Lewis, D. G. Nocera, *Proc. Natl. Acad. Sci. U.S.A* **2006**, *103*, 15729-15735; e) N. Armaroli, V. Balzani, *ChemSusChem* **2011**, *4*, 21-36; f) U. Eberle, M. Felderhoff, F. Schüth, *Angew. Chem Int. Ed.* **2009**, *48*, 6608-6630.

- [6] R. Tanaka, M. Yamashita, L. W. Chung, K. Morokuma, K. Nozaki, *Organometallics* **2011**, *30*, 6742-6750.
- [7] a) P. G. Jessop, Y. Hsiao, T. Ikariya, R. Noyori, *J. Am. Chem. Soc.* **1996**, *118*, 344-355; b) F. Joó, F. Joó, L. Nádasdi, J. Elek, G. Laurenczy, L. Nádasdi, *Chem. Commun.* **1999**, 971-972; c) H. Hayashi, S. Ogo, S. Fukuzumi, *Chem. Commun.* **2004**, 2714-2715; d) Y. Himeda, N. Onozawa-Komatsuzaki, H. Sugihara, H. Arakawa, K. Kasuga, *Organometallics* **2004**, *23*, 1480-1483; e) Y. Himeda, N. Onozawa-Komatsuzaki, H. Sugihara, K. Kasuga, *Organometallics* **2007**, *26*, 702-712; f) R. Tanaka, M. Yamashita, K. Nozaki, *J. Am. Chem. Soc.* **2009**, *131*, 14168-14169; g) T. J. Schmeier, G. E. Dobereiner, R. H. Crabtree, N. Hazari, *J. Am. Chem. Soc.* **2011**, *133*, 9274-9277; h) M. S. Jeletic, M. T. Mock, A. M. Appel, J. C. Linehan, *J. Am. Chem. Soc.* **2013**, *135*, 11533-11536; i) C. A. Huff, M. S. Sanford, *ACS Catal.* **2013**, *3*, 2412-2416; j) G. A. Filonenko, R. van Putten, E. N. Schulpen, E. J. M. Hensen, E. A. Pidko, *ChemCatChem* **2014**, *6*, 1526-1530; k) J. Kothandaraman, M. Czaun, A. Goeppert, R. Haiges, J.-P. Jones, R. B. May, G. K. S. Prakash, G. A. Olah, *ChemSusChem* **2015**, *8*, 1442-1451; l) F. Bertini, N. Gorgas, B. Stöger, M. Peruzzini, L. F. Veiros, K. Kirchner, L. Gonsalvi, *ACS Catal.* **2016**, *6*, 2889-2893; m) S.-M. Lu, Z. Wang, J. Li, J. Xiao, C. Li, *Green Chem.* **2016**, *18*, 4553-4558; n) R. Kanega, N. Onishi, D. J. Szalda, M. Z. Ertem, J. T. Muckerman, E. Fujita, Y. Himeda, *ACS Catal.* **2017**, *7*, 6426-6429.
- [8] a) C. Fellay, P. J. Dyson, G. Laurenczy, *Angew. Chem Int. Ed.* **2008**, *47*, 3966-3968; b) B. Loges, A. Boddien, H. Junge, M. Beller, *Angew. Chem Int. Ed.* **2008**, *47*, 3962-3965; c) Y. Himeda, *Green Chem.* **2009**, *11*, 2018-2022; d) J. H. Barnard, C. Wang, N. G. Berry, J. Xiao, *Chem. Sci.* **2013**, *4*, 1234-1244; e) E. A. Bielinski, P. O. Lagaditis, Y. Zhang, B. Q. Mercado, C. Würtele, W. H. Bernskoetter, N. Hazari, S. Schneider, *J. Am. Chem. Soc.* **2014**, *136*, 10234-10237; f) S. Oldenhof, M. Lutz, B. de Bruin, J. Ivar van der Vlugt, J. N. H. Reek, *Chem. Sci.* **2015**, *6*, 1027-1034; g) I. Mellone, N. Gorgas, F. Bertini, M. Peruzzini, K. Kirchner, L. Gonsalvi, *Organometallics* **2016**, *35*, 3344-3349; h) S.-M. Lu, Z. Wang, J. Wang, J. Li, C. Li, *Green Chem.* **2018**, *20*, 1835-1840; i) N. Lentz, M. Albrecht, *ACS Catal.* **2022**, *12*, 12627-12631; j) J. Guo, M. Li, C. Yin, D. Zhong, Y. Zhang, X. Li, Y. Wang, J. Yuan, H. Xie, T. Qi, *Inorg. Chem.* **2023**, *62*, 18982-18989; k) L. Guo, Z. Li, M. Cordier, R. Marchal, B. Le Guennic, C. Fischmeister, *ACS Catal.* **2023**, *13*, 13626-13637; l) S. Cheng, Z. Lang, J. Du, Z. Du, Y. Li, H. Tan, Y. Li, *Journal of Catalysis* **2022**, *413*, 119-126; m) S. Ge, L. Gong, P. Yi, X. Mo, C. Liu, X.-Y. Yi, P. He, *Inorg. Chem.* **2023**, *62*, 18375-18383; n) G. M. Rodriguez, F. Zaccaria, L. Tensi, C. Zuccaccia, P. Belanzoni, A. Macchioni, *Chem.-Eur. J.* **2021**, *27*, 2050-2064; o) C. Fink, G. Laurenczy, *Dalton Trans.* **2017**, *46*, 1670-1676; p) S. Patra, H. Deka, S. K. Singh, *Inorg. Chem.* **2021**, *60*, 14275-14285; q) S. Patra, S. K. Singh, *Inorg. Chem.* **2020**, *59*, 4234-4243; r) G. M. Rodriguez, C. Domestici, A. Bucci, M. Valentini, C. Zuccaccia, A. Macchioni, *Eur. J. Inorg. Chem.* **2018**, 2247-2250.
- [9] a) A. Boddien, F. Gärtner, C. Federsel, P. Sponholz, D. Mellmann, R. Jackstell, H. Junge, M. Beller, *Angew. Chem Int. Ed.* **2011**, *50*, 6411-6414; b) R. Verron, E. Puig, P. Sutra, A. Igau, C. Fischmeister, *ACS Catal.* **2023**, *13*, 5787-5794; c) L. Piccirilli, B. Rabell, R. Padilla, A. Riisager, S. Das, M. Nielsen, *J. Am. Chem. Soc.* **2023**, *145*, 5655-5663; d) Y. Maenaka, T. Suenobu, S. Fukuzumi, *Energy Environ. Sci.* **2012**, *5*, 7360-7367; e) S. Semwal, A. Kumar, J. Choudhury, *Catal. Sci. Technol.* **2018**, *8*, 6137-6142; f) J. Fidalgo, M. Ruiz-Castañeda, G. García-Herbosa, A. Carbayo, F. A. Jalón, A. M. Rodríguez, B. R. Manzano, G. Espino, *Inorg. Chem.* **2018**, *57*, 14186-



- 14198; g) B. Maji, A. Kumar, A. Bhattacherya, J. K. Bera, J. Choudhury, *Organometallics* **2022**, *41*, 3589-3599.
- [10] a) Y. Suna, M. Z. Ertem, W. H. Wang, H. Kambayashi, Y. Manaka, J. T. Muckerman, E. Fujita, Y. Himeda, *Organometallics* **2014**, *33*, 6519-6530; b) W.-H. Wang, S. Xu, Y. Manaka, Y. Suna, H. Kambayashi, J. T. Muckerman, E. Fujita, Y. Himeda, *ChemSusChem* **2014**, *7*, 1976-1983.
- [11] W.-H. Wang, J. F. Hull, J. T. Muckerman, E. Fujita, Y. Himeda, *Energy Environ. Sci.* **2012**, *5*, 7923-7926.
- [12] J. F. Hull, Y. Himeda, W.-H. Wang, B. Hashiguchi, R. Periana, D. J. Szalda, J. T. Muckerman, E. Fujita, *Nat. Chem.* **2012**, *4*, 383-388.
- [13] S. A. Xu, N. Onishi, A. Tsurusaki, Y. Manaka, W. H. Wang, J. T. Muckerman, E. Fujita, Y. Himeda, *Eur. J. Inorg. Chem.* **2015**, 5591-5594.
- [14] N. Onishi, M. Z. Ertem, S. Xu, A. Tsurusaki, Y. Manaka, J. T. Muckerman, E. Fujita, Y. Himeda, *Catal. Sci. Technol.* **2016**, *6*, 988-992.
- [15] L. Wang, N. Onishi, K. Murata, T. Hirose, J. T. Muckerman, E. Fujita, Y. Himeda, *Chemsuschem* **2017**, *10*, 1071-1075.
- [16] a) G. Menendez Rodriguez, A. Bucci, R. Hutchinson, G. Bellachioma, C. Zuccaccia, S. Giovagnoli, H. Idriss, A. Macchioni, *ACS Energy Lett.* **2017**, *2*, 105-110; b) A. Bucci, S. Dunn, G. Bellachioma, G. Menendez Rodriguez, C. Zuccaccia, C. Nervi, A. Macchioni, *ACS Catal.* **2017**, *7*, 7788-7796; c) A. H. Ngo, M. Ibañez, L. H. Do, *Acs Catal.* **2016**, *6*, 2637-2641.
- [17] R. Kanega, M. Z. Ertem, N. Onishi, D. J. Szalda, E. Fujita, Y. Himeda, *Organometallics* **2020**, *39*, 1519-1531.